Dalton Transactions

Gas-phase synthesis of $[O=U-X]^+$ (X= Cl, Br and I) from a UO_2^{2+} precursor using ion-molecule reactions and an $[O=U\equiv CH]^+$ intermediate

Journal:	*Dalton Transactions*
Manuscript ID	DT-COM-08-2023-002811.R1
Article Type:	Paper
Date Submitted by the Author:	05-Feb-2024
Complete List of Authors:	Terhorst, Justin; Duquesne University Bayer School of Natural and Environmental Sciences Lenze, Samuel; Duquesne University Bayer School of Natural and Environmental Sciences Metzler, Luke; Duquesne University Bayer School of Natural and Environmental Sciences, Fry, Allison; Duquesne University Bayer School of Natural and Environmental Sciences Ihabi, Amina; Duquesne University Bayer School of Natural and Environmental Sciences Corcovilos, Theodore A.; Duquesne University, Physics van Stipdonk, Michael; Duquesne University Bayer School of Natural and Environmental Sciences, Chemistry and Biochemistry

ARTICLE

Gas-phase synthesis of $[O=U-X]^+$ (X= Cl, Br and I) from a UO_2^{2+} precursor using ion-molecule reactions and an $[O=U\equiv CH]^+$ intermediate

Received 00th January 20xx,
Accepted 00th January 20xx

DOI: 10.1039/x0xx00000x

Justin Terhorst[a], Samuel Lenze[a], Luke Metzler[a‡], Allison N. Fry[a†], Amina Ihabi[a], Theodore A. Corcovilos[b] and Michael J. Van Stipdonk[a*]

Difficulty in the preparation of gas-phase ions that include U in middle oxidation states (III,IV) have hampered efforts to investigate intrinsic structure, bonding and reactivity of model species. Our group has used preparative tandem mass spectrometry (PTMS) to synthesize a gas-phase U-methylidyne species, $[O=U\equiv CH]^+$, by elimination of CO from $[UO_2(C\equiv CH)]^+$ [*J. Am. Soc. Mass Spectrom.* 30, 796–805 (2019)], which has been used as an intermediate to create products such as $[OUN]^+$ and $[OUS]^+$ by ion-molecule reactions. Here, we investigated the reactions of $[O=U\equiv CH]^+$ with a range of alkyl halides to determine whether the methylidyne is a also a useful intermediate for production and study of the oxy-halide ions $[OUX]^+$, where X=Cl, Br and I, formally U(IV) species for which intrinsic reactivity data is relatively scarce. Our experiments demonstrate that $[OUX]^+$ is the dominant product ion generated by reaction $[O=U\equiv CH]^+$ with neutral regents such as CH_3Cl, CH_3CH_2Br and $CH_2=CHCH_2I$.

Introduction

Electrospray ionization (ESI) has proved effective for generation of gas-phase complex ions built upon a uranyl ($UO_2^{+/2+}$) moiety[1-4]. Recently, several studies have shown that the notoriously stable axial U=O bonds of UO_2^{2+} can be activated in preparative tandem mass spectrometry ($PTMS^n$) experiments via collision induced dissociation (CID). The term "preparative" designates that the reactants are generated *in situ* using CID and/or ion-molecule reactions of precursors using a series of discrete MS^n steps before the target reactions occur. Activation of UO_2^{2+} ultimately facilitates substitution or elimination of one or more "yl" oxo ligands, enabling the generation of a myriad of novel U-containing ions in the gas phase where the intrinsic ion-molecule reactivity may be studied[5]. In essence, by preparing reactive U species in the gas-phase using $PTMS^n$, fundamental questions concerning the chemistry may be studied without complicating condensed-phase influences. This information used in conjunction with complementary state of the art quantum chemical computations give a powerful technique which can be utilized to uncover reactivity trends, hence helping to develop a larger theory of actinide-based chemistry. Specifically, U species that can be generated and investigated in the gas-phase for which there are little to no experimental data concerning their reactivity may uncover trends that motivate efforts to synthesize them or similar molecules in the condensed-phase.

For example, in a previous study, our group discovered that the nitrido species $[NUO]^+$ can be created by rearrangement of $[UO_2(N\equiv C)]^+$ followed by elimination of CO; illustrating an example of the loss of an oxo ligand from $UO_2^{+/2+}$.[5c] In general, the gas-phase oxo-elimination reactions appear to be thermochemically driven by: rearrangement, formation of C-O and N-O bonds that include the axial O atoms of UO_2, and or the loss of small neutral molecules such as CO_2,[5a] N_2,[5b] and CO.[5c,5e,5g]

While there are many studies of the gas-phase reactions of U(VI) and U(V) species using ESI and tandem mass spectrometry, there are far fewer reports on the preparation and study of gas-phase ions that include U in the middle oxidation states (III,IV). Investigations of species with U(III or IV) would significantly enhance the understanding of intrinsic uranium chemistry and is the motivation of this study. The ability to activate and substitute the oxo ligands of UO_2^{2+} in the gas-phase provides a gateway for the creation of formally U(III) and U(IV) species for intrinsic chemistry studies. Recently, we have demonstrated that $PTMS^n$ experiments initiated with solvent-coordinated $[UO_2(O_2C\text{-}C\equiv CH)]^+$ (generated by ESI) can be used to prepare the organometallic species, $[UO_2(C\equiv CH)]^+$, by decarboxylation[5g]. High-accuracy *m/z* measurements demonstrated conclusively that subsequent CID of $[UO_2(C\equiv CH)]^+$ drives an unprecedented gas-phase rearrangement reaction which leads to elimination of CO and creation of $[OUCH]^+$. Relative energies for various possible structures produced by density functional theory (DFT)

[a] *Department of Chemistry and Biochemistry, Duquesne University, Pittsburgh PA 15282 USA*
[b] *Department of Physics, Duquesne University, Pittsburgh PA 15282 USA*
† Current address: Department of Chemistry, University of North Carolina at Chapel Hill, Chapel Hill, NC 27599-3290
‡ Current address: Ardara Technologies L.P., Ardara, PA 15615
* To whom correspondence should be addressed
Electronic Supplementary Information (ESI) available: [details of any supplementary information available should be included here]. See DOI: 10.1039/x0xx00000x

calculations, assessments of molecular orbitals, and bonding, all suggested that the $[O=U\equiv CH]^+$ ion is a uranium-methylidyne product[5g]. Subsequent experiments showed that $[O=U\equiv CH]^+$ reacts spontaneously with H_2O to create $[UO_2]^+$, through a series of H-transfer steps to create an $[UO_2(CH_3)]^+$ intermediate and subsequent elimination of methyl radical[5j]. Additionally, the $[O=U\equiv CH]^+$ ion has shown to react spontaneously with $CH_3C\equiv N$ to create $[NUO]^+$,[5j] and with CS_2 to generate $[OUS]^+$ [5k] in previous studies by our group.

The high reactivity of $[O=U\equiv CH]^+$, exhibited in our earlier studies led us to consider whether the species might be used as an intermediate for "synthesis" of novel middle oxidation state U-containing ions for gas-phase studies. Here, we report an experimental investigation of the reaction of $[O=U\equiv CH]^+$ with a range of neutral alkyl-halide reagents in a modified linear ion trap instrument. Our hypothesis was that the reaction with alkyl-halides would generate the U(IV) ion,$[OUX]^+$, (where X is the halogen substituent from the alkyl-halide reagent) via metathesis. While halide substituted U species such as OUF_2 and $N\equiv UF_3$ have been generated in matrix isolation studies,[6,7] or by reactions of U^+ with neutral reagents,[8] this study probed whether the series of related ions can be generated starting from $UO_2^{+/2+}$ precursors using $PTMS^n$ for subsequent ion-molecule reactivity investigation.

Experimental Methods

Sample Preparation

Methanol (CH_3OH), dichloromethane (CH_2Cl_2), chloroform ($CHCl_3$), bromomethane, dibromomethane, bromoethane, allyl-bromide (CH_2=CH-CH_2Br), iodomethane (CH_3I), di-idomethane (CH_2I_2), iodoethane (ICH_2CH_3) and allyl-iodide (CH_2=CH-CH_2I) were purchased from Sigma-Aldrich Chemical (St. Louis, MO) and used as received. A sample of uranyl propiolate was prepared as described previously by combining 2–3 mg of $U^{VI}O_3$ (Strem Chemicals, Newburyport MA), corresponding to approximately 7×10^{-6} to 1×10^{-5} moles, with 2–3 mL of propiolic acid (HO_2C-C≡CH, Sigma Aldrich, St. Louis MO) and 400 mL of deionized/distilled H_2O in a glass scintillation vial. *Caution: uranium oxide is radioactive (a- and g-emitter), and proper shielding, waste disposal and personal protective gear should be used when handling the material*.

Mass Spectrometry Experiments

Electrospray ionization (ESI) and CID experiments were performed on a ThermoScientific (San Jose, CA) LTQ-XL linear ion trap (LIT) mass spectrometer. A solution of uranyl propiolate in 80/20 (v:v) H_2O/CH_3OH for ESI was infused into the instrument using the incorporated syringe pump at a flow rate of 5 mL/min. The atmospheric pressure ionization stack settings of the LTQ-XL (lens voltages, quadrupole and octopole voltage offsets, etc.) were optimized for maximum transmission of precursor ions to the ion trap using the auto-tune routine within the LTQ Tune program. Helium was used as the bath/buffer gas.

For multiple-stage (MS^n) CID experiments, the $[UO_2(O_2C$-C≡CH)$(CH_3OH)_2]^+$ precursor ion used to prepare $[OUCH]^+$ by tandem MS, was isolated using a width of 1.0 to 1.5 mass to charge (*m/z*) units. The exact value was determined empirically to provide maximum ion intensity while ensuring isolation of a single isotopic peak. Similar ion isolation parameters were used for subsequent CID steps. The (mass) normalized collision energy (NCE, as defined by ThermoScientific) was set between 5 and 18%, which corresponds to 0.075–0.27 V applied for CID with the current instrument calibration. The activation Q, which defines the frequency of the applied radio frequency potential, was set at 0.30 and a 30 ms activation time was used.

The linear ion trap has been modified to allow the mixing of neutral liquid and gaseous reagents with the helium buffer gas before introduction into the ion trap[5h]. Liquid reagents are introduced into the manifold from a metered syringe pump, where they evaporate. The partial pressure of these reagents may be controlled through the syringe pump rate, the helium flow rate, and by heating or cooling the manifold, which is done by wrapping the manifold tubing with a temperature-controlled water coil. All gas ports are controlled by manually actuated precision needle valves, which provide control of the flow rates. To probe gas-phase reactions of $[O=U\equiv CH]^+$ with background neutrals, ions were isolated using widths of 1–2 *m/z* units. Here too, the specific width used was chosen empirically to ensure maximum ion isolation efficiency. The ions were then stored in the LIT for periods ranging from 1 ms to 10 s. When examining ion-molecule reactions (IMRs), our intent was not to measure or report rates or rate constants, but to identify the *pathways* by which ions react with alkyl halide neutrals in the LIT. The specific isolation times were used to demonstrate the general changes in precursor and product ion intensities as isolation time is varied and confirm that specific ions are created by bimolecular reactions in the ion trap. Because the experiments were performed using the multi-dimensional tandem mass spectrometry capabilities of the linear ion trap, care had to be taken to ensure that enough neutral reagent was present in the ion trap for ion-molecule reaction studies, without hampering the synthesis of reactive species using multiple initial CID steps in series. For both CID and IMR experiments, the mass spectra displayed were created by accumulating and averaging at least 30 isolation, dissociation, and ejection/detection steps.

Computational Methodology

Kohn-Sham DFT computations were performed using the *Gaussian16* quantum chemistry package[9a]. For uranium and iodine, the Stuttgart Dresden basis set (SDD-VDZ-MWB) with its accompanying small-core quasi-relativistic effective core potential (MWB60) was employed[9b]. A triple-ζ with diffuse function Pople basis set, 6-311+g(d,p), was used for the rest of the elements in the system. The structures of the reaction reactants, intermediates, transition states, and products were optimized using two different density functionals, B3LYP [9c] and PBE0 (PBE1PBE)[9d]. The choice of the density functionals and basis sets were made in retrospect of the good performance in previous computational studies involving uranium oxides and related species[9e]. All the reported transition states were confirmed by intrinsic reaction coordinate (IRC) calculations. There is a reasonable agreement between the

relative energies obtained at B3LYP and PBE0 functionals; the largest difference in relative energies is *ca*. 22.3 kJ/mol. Singlet-state calculations were performed using the restricted Kohn-Sham formalism, whereas triplet-state species were calculated utilizing the unrestricted approach. Although it is feasible that the energies of the reaction intermediates and transition states involving species having different uranium oxidation states could be affected by the inclusion of spin-orbit corrections; this detail does not substantially affect the critical interpretations gleaned from the computed relative energies. Potential energy surfaces and additional computational detail of the reactions discussed herein are shown in the supporting information.

Results and Discussion

Reactions of $[OUCH]^+$ with alkyl halides

Production of $[O=U\equiv CH]^+$ using $PTMS^n$ has been described in detail elsewhere[5g], and the same approach was used in the present study. Briefly, a methanol-coordinated uranyl (UO_2^{2+}) propiolate cation, $[UO_2(O_2C\text{-}C\equiv CH)(CH_3OH)_2]^+$, was created via ESI using a sample of uranyl propiolate synthesized *in situ*. $PTMS^n$ experiments were performed on a quadrupole ion trap mass spectrometer modified to allow introduction of neutral reagents for studies of ion-molecule reactivity.

Before delving into the details of each experiment described here, it should be noted that the $[O=U\equiv CH]^+$ ion (*m/z* 267) is converted to UO_2^+ (*m/z* 270) by reactions with either H_2O and O_2 (Figure 1), which are common background molecules in the ion trap mass spectrometer[5j]. The reaction of $[O=U\equiv CH]^+$ with H_2O and O_2 have been explored in detail in our earlier study[5j]. For the sake of comparison to data discussed below, the product ion spectra generated by reaction of $[O=U\equiv CH]^+$ with background species in the ion trap (no deliberate introduction of neutral reagent) for periods ranging from 1 ms to 100 ms are provided in Figure S1 of the supporting information.

The first experiment performed for this study was the reaction of $[OUCH]^+$ with CH_3I. As described previously, the working hypothesis was the creation of $[OUI]^+$ from this reaction. Product ion spectra generated by reaction of $[O=U\equiv CH]^+$ (*m/z* 267) with CH_3I are provided in Figure 1a–c. The relative abundance of $[O=U\equiv CH]^+$ decreases with increasing isolation/reaction time, and the appearance and increase in relative abundance of a product ion at *m/z* 381 is consistent with the metathesis of the methylidyne (CH) ligand with I by reaction 1. This observation supported the hypothesis that novel U(IV) ($[OUX]^+$) species can be generated using $PTMS^n$ and the reactive $[O=U\equiv CH]^+$ ion.

(1) $[O=U\equiv CH]^+ + CH_3I \rightarrow [O=U\text{-}I]^+ + C_2H_4$

We note that the neutral reaction products cannot be observed using the ion trap but can be inferred from the missing mass and corroboration of the proposed reaction mechanisms using density functional theory (DFT) simulations, as described in the "Computational Results" section below. In addition, ion trap mass spectrometry cannot distinguish among isomers of either the ions or neutral products, but DFT can be used to identify likely products and conformations.

The next logical step was to modify the introduced reagent by changing the alkyl group to test for similar reactivity, hence CH_3CH_2I was used. The product ion spectra generated by reaction of $[O=U\equiv CH]^+$ with CH_3CH_2I are provided in Figure 2a–c. In this case, the isolation of $[O=U\equiv CH]^+$, without imposed collisional activation, for periods of 10 ms and 100 ms (Fig. 2a and 2b, respectively) leads to a decrease in relative abundance of $[O=U\equiv CH]^+$, and the rise in relative abundance of product ions at *m/z* 381 and *m/z* 395. The former is consistent with generation of $[OUI]^+$, which the latter is attributed to creation of $[OUCH_2I]^+$. Interestingly, subsequent CID of $[OUCH_2I]^+$ (Fig. 2c) caused the elimination of 127 Da (I●) to produce $[OU=CH_2]^+$. This observation is noteworthy in the context of the desire to synthesize and characterize species with U-C multiple bonds. In our previous study[5j], gas-phase data strongly suggests that CID of $[UO_2(C\equiv CH)]^+$ creates the oxouranium methylidyne $[O=U\equiv CH]^+$. The observation of product ions at *m/z* 286 in Figure 2c suggests the formation of an analogous oxouranium methylidene.

The additional reactions investigated are summarized in Table 1. The formally U(IV) ions $[OUX]^+$, X=Cl, Br and I are generated in relatively high abundance when $[O=U\equiv CH]^+$ is allowed to react with neutral reagents such as CH_3Cl, CH_2Cl_2, CH_3CH_2Br, CH_3I, CH_3CH_2I and $CH_2{=}CHCH_2I$ that are deliberately mixed with the He bath gas of the ion trap. The fact that the $[OUX]^+$ species are created without the need for imposed collisional activation suggests that they are created by a spontaneous reaction pathway. From the observations and conclusions of this study, we hypothesize that $[OUF]^+$ can be generated using reactions of $[O=U\equiv CH]^+$ with fluorocarbons such as CF_4. However, we have shown that $[OUF]^+$ can be

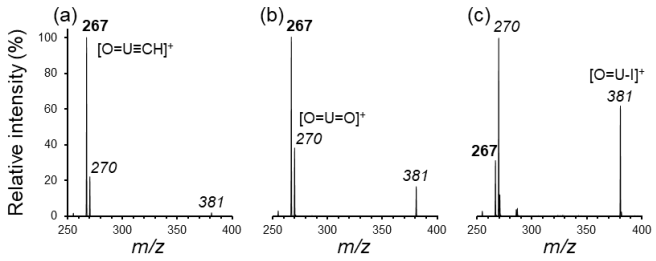

Figure 1 Product ion spectra generated by isolation (MS^5 stage) of $[OUCH]^+$ (*m/z* 267) for reaction with iodomethane (CH_3I): (a) 1 ms reaction time, (b) 10 ms reaction time and (c) 100 ms reaction time. In the figure, precursor ion is indicated with bold font and reaction products identified with italicized font.

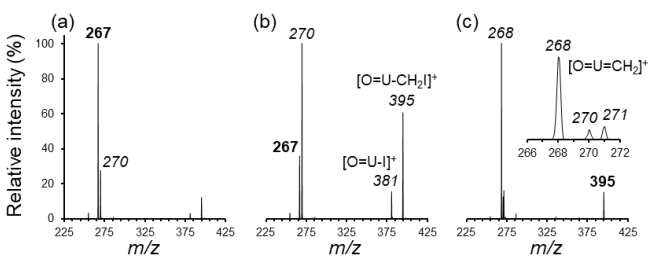

Figure 2 Product ion spectra generated by isolation (MS^5 stage) of $[OUCH]^+$ (*m/z* 267) for reaction with iodoethane (CH_3H_2I): (a) 1 ms reaction time, (b) 10 ms reaction time and (c) 100 ms reaction time. In the figure, precursor ion is indicated with bold font and reaction products identified with italicized font.

Table 1 Ion molecule reactions investigated in this set of experiments.

(1)	$[OUCH]^+ + CH_2Cl_2 \rightarrow [OUCl]^+ + C_2H_3Cl°$
(2)	$[OUCH]^+ + CHCl_3 \rightarrow [OUCl]^+ + C_2H_2Cl_2°$
(3)	$[OUCH]^+ + CH_2Br_2 \rightarrow [OUBr]^+ + C_2H_3Br°$
(4)	$[OUCH]^+ + CH_3CH_2Br \rightarrow [OUBr]^+ + C_3H_6°$
(5)	$[OUCH]^+ + CH_3CH_2Br \rightarrow [OUCH_2Br]^+ + C_2H_4°$
(6)	$[OUCH]^+ + CH_2{=}CHCH_2Br \rightarrow [OUBr]^+ + C_4H_6°$
(7)	$[OUCH]^+ + CH_3I \rightarrow [OUI]^+ + C_2H_4°$
(8)	$[OUCH]^+ + CH_2I_2 \rightarrow [OUI]^+ + C_2H_3I°$
(9)	$[OUCH]^+ + CH_3CH_2I \rightarrow [OUI]^+ + C_3H_6°$
(10)	$[OUCH]^+ + CH_3CH_2I \rightarrow [OUCH_2I]^+ + C_2H_4°$
(11)	$[OUCH]^+ + CH_2{=}CHCH_2I \rightarrow [OUI]^+ + C_4H_6°$

For each reaction, the $[O{=}U{\equiv}CH]^+$ "reagent ion" was created by $PTMS^n$ from a $[UO_2(O_2C\text{-}C{\equiv}CH)(CH_3OH)_2]^+$ precursor ion generated by electrospray ionization.

generated from an alternative precursor ion and without the need for an ion-molecule reaction[5h]. Using a $[UO_2(C_6F_5)]^+$ ion generated using $PTMS^n$, the reaction of $[UO_2(C_6F_5)]^+$ with H_2O illustrates the substitution of OH for F to create $[UO_3HC_6F_4]^+$, which is favored over hydrolysis to produce $[UO_2(OH)]^+$ and (neutral) C_6F_5H. Subsequent CID of $[UO_3HC_6F_4]^+$ generates $[UO_2(F)]^+$ and $[OUF]^+$. This result demonstrates that a homologous group of $[OUX]^+$ cations can be generated in the gas-phase using $PTMS^n$ using a different precursor ion containing a UO_2^{2+} moiety.

By mixing a second neutral reagent with the alkyl-halide prior to introduction into the ion trap, the product ions generated by subsequent reaction(s) of $[O{=}U\text{-}X]^+$ could be investigated. For example, we found that $[O{=}U\text{-}I]^+$ reacts with H_2O to generate $[O{=}U\text{-}OH]^+$ at *m/z* 271 (reaction 2, and Figure S2 of the supporting information), which subsequently reacts with a second H_2O molecule to create $[UO_2OH]^+$ at *m/z* 287. Reaction of $[O{=}U\text{-}I]^+$ with CH_3OH leads to formation of $[O{=}U\text{-}OCH_3]^+$ at *m/z* 285 (Figure S3b of the supporting information).

(2) $[O{=}U\text{-}I]^+ + H_2O \rightarrow [O{=}U\text{-}OH]^+ + HI$

These results demonstrate that the $PTMS^n$ approach provides the opportunity to examine the intrinsic reactivity of the novel $[O{=}U\text{-}X]^+$ and related species after their creation *in situ*.

(3) $[O{=}U\text{-}I]^+ + CH_3OH \rightarrow [O{=}U\text{-}OCH_3]^+ + HI$

Computational Results

To probe the pathway by which the $[O{=}U\text{-}X]^+$ species is formed, DFT calculations were used to identify potential minima, transition state structures, and their relative energies using reaction of $[O{=}U{\equiv}CH]^+$ with CH_3I as the model. Figure 3 shows the reaction energy diagram for a step-wise process that leads to creation of $[OUI]^+$. Formation of the encounter complex (structure **II**) is predicted to be exothermic by *ca.* 118 kJ/mol. Transfer of H from CH_3I to the alkylidyne ligand is calculated to create intermediate **III**, an oxouranium methylidene coordinated by CH_2I, through the predicted transition state structure **TSII→III**. Concerted formation of $CH_2{=}CH_2$ and cleavage of the CH_2-I bond is calculated to then create an ion-molecule complex between $[OUI]^+$ and $CH_2{=}CH_2$ (structure **IV**) through transition state **TSIII→IV**. Elimination of $CH_2{=}CH_2$ creates $[OUI]^+$. The computed reaction energies show that formation of $[OUI]^+$ via the reaction of $[OUCH]^+$ with CH_3I is exothermic and spontaneous, which agreed with the experimental observation. The pathway depicted in Figure 3 also indicated that the reaction involves crossing of the singlet to triplet energy surface between **III** and **TSIII→IV** to create $[OUI]^+$ in the triplet spin state. Additionally, a second pathway was identified (Figure S4 of the supporting information) that involves insertion of the alkylidyne ligand into the CH_3-I bond to create an intermediate (structure **V**, Figure S4) composed of an oxouranium alkylidene coordinated by an ethenyl ligand. Subsequent intramolecular proton transfer would create the ethene-coordinated $[OUI]^+$ species. However, on both the singlet and triplet surfaces, the transition state for the insertion step (**TSII→V**, Figure S4) lies 33–84 kJ/mol above the energy of reactants ($[OUCH]^+$ and CH_3I), thus suggesting that there is a barrier to this reaction along this pathway.

Preliminary DFT calculations suggested that the intrinsic structure of $[OUX]^+$ is linear, with the triplet state favored over the singlet state. Species such as $[OUOH]^+$ and $[OUOCH_3]^+$ are also predicted to have linear structures. For $[OUF]^+$, $[OUCl]^+$, $[OUBr]^+$ and $[OUI]^+$, vibrational frequency calculations predict a subtle red shift of the U=O stretching frequency progressing

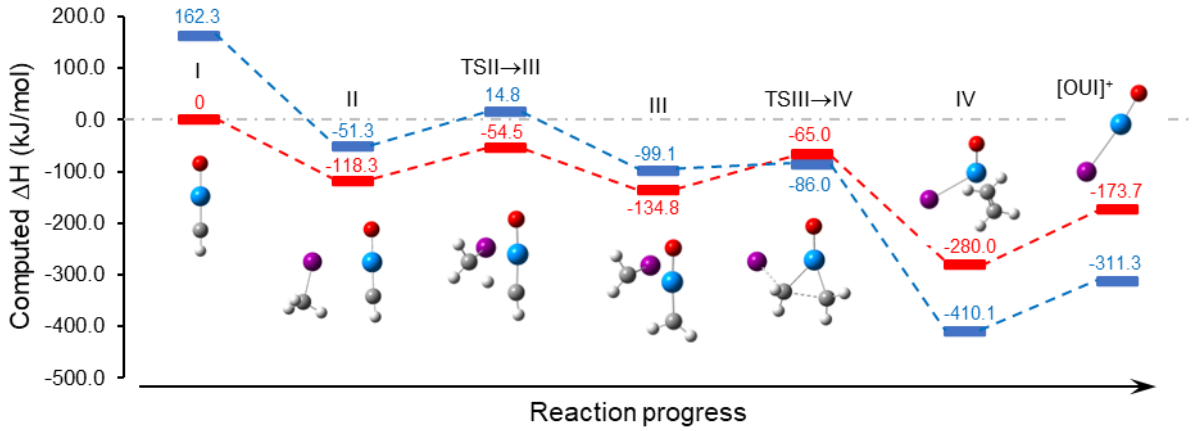

Figure 3 Reaction energy diagram for the reaction of $[OUCH]^+$ with CH_3I via pathway 1, as outlined in the text. Data in blue represents structures (minima and transition states) in the singlet spin state. Species in the triplet spin state are indicated in red. Data generated by the PBE0/SDD/6-311+G(d,p) level of theory.

from X=I to X=F; consistent with earlier computational and ion spectroscopy investigations of ions such as $[UO_2(X)_3]^-$.[9]

Conclusions

To summarize, we have shown that $PTMS^n$ can be used to convert UO_2^{2+} to formally U(IV) oxy-halide ions $[O=U-X]^+$, where X=Cl, Br and I, and related species for studies of intrinsic reactivity. The significant advantage of our approach ($PTMS^n$) is the ability to dissociate oxo ligands from a $UO_2^{+/2+}$ moiety to create highly reactive intermediates. These intermediates, such as $[O=U\equiv CH]^+$, can be used as a "gateway" to generate novel U(IV) species described here, in addition to other middle oxidation state U(III and IV) ions. Future studies enabled by this work include investigations of the reactivity of species with putative U-C triple and double bonds, and the role of substituents on the inverse trans influence in formally U(IV) species such as $[O=U-X]^+$.

Author Contributions

JT: investigation, methodology and validation writing – review and editing. SL: investigation and methodology. LM: investigation and methodology. AF: investigation and methodology. AI: investigation and methodology. TAC: conceptualization, methodology, writing – review and editing. MJV: conceptualization, methodology, writing – original draft, project administration.

Conflicts of interest

There are no conflicts to declare.

Acknowledgements

M.V.S. and T.A.C. acknowledge support for this work from the School of Science and Engineering at Duquesne University. Laboratory space renovation partial support for this work by the National Science Foundation (CHE-0963450 and CHE-1950585) is also acknowledged.

Notes and references

1 (*a*) M. Van Stipdonk, G. Gresham, G. Groenewold, V. Anbalagan, D. Hanna, W. Chien, *J. Am. Soc. Mass Spectrom*. 2003, **14**, 1205-1214; (*b*) M. Van Stipdonk, W. Chien, V. Anbalagan, K. Bulleigh, D. Hanna, G. Groenewold, *J. Phys. Chem. A*., 2004, **108**, 10448-10457; (*c*) M. Van Stipdonk, W. Chien, K. Bulleigh, Q. Wu, G. Groenewold, *J. Phys. Chem. A*. 2006, **110**, 959-970; (*d*) V. Anbalagan, W. Chien, G. L. Gresham, G. S. Groenewold, M. J. Van Stipdonk. *Rapid Commun. Mass Spectrom*. 2004, **18**, 3028-3034; (*e*) D. Rios, P. X. Rutkowski, M. J. Van Stipdonk, J. K. Gibson. *Inorg. Chem.* 2011, **50**, 4781-4790; (*f*) M. Van Stipdonk, M. Michelini, A. Plaviak, D. Martin, J. Gibson, *J. Phys. Chem. A*. 2014, **118**, 7838-7846; (*g*) M. J. Van Stipdonk, C. O'Malley, A. Plaviak, D. Martin, J. Pestok, P. A. Mihm, C. G. Hanley, T. A. Corcovilos, J. K. Gibson, B. J. Bythell. *Int. J. Mass Spectrom*. 2016, **396**, 22-34; (*h*) E. Perez, C. Hanley, S. Koehler, J. Pestok, N. Polonsky, M. Van Stipdonk, *J. Am. Soc. Mass Spectrom*. 2016, **27**, 1989-1998; (*i*) M. J. Van Stipdonk, A. Iacovino, I. Tatosian. *J. Am. Soc. Mass Spectrom*. 2018, **29**, 1416-1424.

2 (*a*) V. Rodriguez, P. Burns, *Chem. Eur. J*. 2023, **29**, e202300794; (*b*) V. Rodriguez, H. Culbertson, G. Sigmon, P. Burns, *Inorg. Chem*. 2023, **62**, 4456-4466; (*c*) S. Hickam, S. Aksenov, M. Dembowski, S. Perry, H. Traustason, M. Russell, P. Burns, *Inorg. Chem*. 2018, **57**, 9296-9305.

3 X.-H. Kong, Q.-Y. Wu, X.-R. Zhang, C. Wang, K.-Q. Hu, Z.-F. Chai, C.-M. Nie, W.Q. Shi, *J. of Mol. Liq*., 2020, **300**, 112287; (*b*) K. George, J. Muller, L. Berthon, C. Berthon, D. Guillaumont, I. Vitorica-Yrezabal, H. V. Stafford, L. Natrajan, C. Tamain, *Inorg. Chem*. 2019, **58**, 6904-6917; (*c*) H. Brinkmann, M. Patzschke, P. Kaden, M. Raiwa, A. Rossberg, R, Kloditz, K. Heim, H. Moll, T. Stumpf, *Dalton Trans*, 2019, **48**, 13440-13457; (*d*) C. Zarzana, G. Groenewold, M. Benson, J. Delmore, T. Tsuda, R. Hagiwara, *J. Am. Soc. Mass Spectrom*., 2018, **29**, 1963-1970; (*e*) A. Davis, B. Clowers, *Talanta*, 2018, **176**, 140-150; (*f*) Z. Qin, S. Shi, C. Yang, J. Wen, J. Jia, X. Zhang, H. Yu, X. Wang, *Dalton Trans*., 2016, **45**, 16413-16421; (*g*) Z. Xiong, M. Yang, X. Chen, Y. Gong, Yu. *Inorg. Chem*., 2023, **62**, 2266-2272; (*h*) Z. Xiong, X. Chen, Y. Gong, *Phys. Chem. Chem. Phys*., 2021, **23**, 20073-20079.

4 (*a*) A. Lucena, L. Maria, J. Gibson, J. Marcalo, *Appl. Sci*., 2023, **13**, 3834; (*b*) T. Jian, M. Vasiliu, Z. Lee, Z. Zhang, D. Dixon, J. Gibson, *J. Phys. Chem. A*, 2022, **126**, 7695-7708; (*c*) A. Lucena, J. Carretas, J. Marcalo, M. Michelini, Y. Gong, J. Gibson, *J. Phys. Chem. A*, 2015, **119**, 3628-3635.

5 (*a*) Y. Gong, V. Vallet, M. Michelini, D. Rios, J. K. Gibson, J. *Phys. Chem. A*. 2014, **118**, 325–330; (*b*) Y. Gong, W. A.; de Jong, J. K. Gibson, *J. Am. Chem. Soc*., 2015, **137**, 5911–5915; (*c*) M. Van Stipdonk, M. Michelini, A. Plaviak, D. Martin, J. Gibson, *J. Phys. Chem. A*. 2014, **118**, 7838–7846; (*d*) P. Dau, P. Armentrout, M. Michelini, J. Gibson. *Phys. Chem. Chem. Phys*. 2016, **18**, 7334–7340; (*e*) R. A. Abergel, W. A. de Jong, G. J-P. Deblonde, P. D. Dau, I. Captain, T. M. Eaton, J. Jian, M. J. van Stipdonk, J. Martens, G. Berden, J. Oomens, J. Gibson, *Inorg. Chem*. 2017, **56**, 12930–12937; (*f*) S.-X. Hu, J. Jian, J. Li, J. K. Gibson, *Inorg. Chem*., 2019, **58**, 10148–10159; (*g*) M. J. van Stipdonk, I. J. Tatosian, A. C. Iacovino, A. R. Bubas, L. Metzler, M. C. Sherman, A. Somogyi, *J. Am. Soc. Mass Spectrom*., 2019, **30**, 796–805; (*h*) M. J. Van Stipdonk, E. H. Perez, L. J. Metzler, A. R. Bubas, T. Corcovilos and A. Somogyi. *Phys. Chem. Chem. Phys*. 2021, **23**, 11844–11851; (*i*) E. H. Perez, I. Tatosian, A. Bubas, S. Kline, L. Metzler, A. Somogyi and M. J. Van Stipdonk. *Int. J. Mass Spectrom*. 2021, **469**, 116664; (*j*) L. J. Metzler, C. T. Farmen, T. A. Corcovilos, M. J. Van Stipdonk. *Phys. Chem. Chem. Phys*. 2021, **23**, 4475–4479; (*k*) L. J. Metzler, C. T. Farmen, A. N. Fry, M. P. Seibert, K. A. Massari, T. A. Corcovilos, M. J. van Stipdonk. *Rapid Commun. Mass Spectrom*. 2022, **36**, e9260.

6 Y. Gong, X. Wang, L. Andrews, T. Schlöder, S. Riedel, *Inorg. Chem*. 2012, **51**, 6983 – 6991.

7 L. Andrews, W. Xuefeng, R. Lindh, B. Roos, C. J. Marsden, *Agnew. Chem. Int. Ed*. 2008, **47**, 5366-5370.

8 A. R. Bubas, C. J. Owens, P. B. Armentrout, *Int. J. Mass Spectrom*. 2022, **472**, 116778.

9 (a) *Gaussian 16*, Revision C.01, M. J. Frisch, G. W. Trucks, H. B. Schlegel, G. E. Scuseria, M. A. Robb, J. R. Cheeseman, G. Scalmani, V. Barone, G. A. Petersson, H. Nakatsuji, X. Li, M. Caricato, A. V. Marenich, J. Bloino, B. G. Janesko, R. Gomperts, B. Mennucci, H. P. Hratchian, J. V. Ortiz, A. F. Izmaylov, J. L. Sonnenberg, D. Williams-Young, F. Ding, F. Lipparini, F. Egidi, J. Goings, B. Peng, A. Petrone, T. Henderson, D. Ranasinghe, V. G. Zakrzewski, J. Gao, N. Rega, G. Zheng, W. Liang, M. Hada, M. Ehara, K. Toyota, R. Fukuda, J. Hasegawa, M. Ishida, T. Nakajima, Y. Honda, O. Kitao, H. Nakai, T. Vreven, K. Throssell,

J. A. Montgomery, Jr., J. E. Peralta, F. Ogliaro, M. J. Bearpark, J. J. Heyd, E. N. Brothers, K. N. Kudin, V. N. Staroverov, T. A. Keith, R. Kobayashi, J. Normand, K. Raghavachari, A. P. Rendell, J. C. Burant, S. S. Iyengar, J. Tomasi, M. Cossi, J. M. Millam, M. Klene, C. Adamo, R. Cammi, J. W. Ochterski, R. L. Martin, K. Morokuma, O. Farkas, J. B. Foresman, and D. J. Fox, Gaussian, Inc., Wallingford CT, 2016. (*b*) A. Weigand, X. Cao, T. Hangele, M. Dolg. *J. Phys. Chem. A* 2014, **118**, 2519–2530. (*c*) P. J. Stephens, F. J. Devlin, C. F. Chabalowski, M. J. Frisch. *J. Phys. Chem*. 1994, **98**, 11623−11627. (*d*) C. Adamo, V. Barone, *J. Chem. Phys*. 1999, **110**, 6158-6170. (*e*) B.B. Averkiev, M. Mantina, R. Valero, I. Infante, A. Kovacs, D.G. Truhlar, L. Gagliardi. *Theor. Chem. Acc*. 2011, **129**, 657–666.